

# A Radiometeorological Study, Part II. An Analysis of VHF Field Strength Variations and Refractive Index Profiles

B. R. Bean, V. R. Frank, and J. A. Lane

Contribution from Central Radio Propagation Laboratory, National Bureau of Standards, Boulder, Colo.

(Received June 7, 1963)

This paper discusses the cumulative probability distributions of field strength for four 200 km VHF paths in Illinois in terms of a classification of refractive index profiles. It is shown that extended elevated layers produce signal enhancements of 10 to 25 db above the level observed in unstratified conditions. Assuming the layer characteristics given by radiosonde data, the best agreement between calculated and measured values of field strength is obtained using a layer model with a linear  $n$ -profile.

The possible influence of smaller layers is also discussed in relation to the observed results for conditions judged to be unstratified or well mixed on the basis of sonde data.

## 1. Introduction

It is evident from the discussion in part I that the further development of radiometeorological parameters would be assisted by a better understanding of the propagation mechanism on non-optical paths. In particular, the influence of thermal stability on signal level, fading rate and wavelength dependence is an important topic requiring further study.

The effect of varying meteorological conditions on signal characteristics is especially marked in the case of paths of "intermediate" length. On such a path the radio field strength in the absence of stable layers or surface ducts will often be comparable with the predicted diffracted field. Furthermore, at frequencies up to say 300 Mc/s ( $\lambda > 1$  m) relatively strong fields will frequently be observed in conditions favorable to the production of temperature inversions in the first 2 km or so above the earth's surface. It is the purpose of this paper to discuss some aspects of radiometeorology relevant to this situation, especially the field strength distribution observed on a 200 km path at frequencies between

72 and 180 Mc/s. The signal characteristics are analyzed in terms of a classification of refractive index profiles, with the objective of clarifying the relative importance of different propagation mechanisms and their influence on the measured field strength distribution.

Table 1 lists characteristic profile types, the assumed mechanism associated with each type, and typical meteorological conditions. Selected references are given for each category, and special mention may be made here of recent work [du Castel, Misme, and Voge, 1960] in France which, to a large extent, unifies and extends earlier analyses based on the separate concepts of "reflection" and "scattering."

## 2. Radio and Meteorological Data

The analysis to follow is limited to paths between Chicago and Urbana, Ill. (fig. 1), since several years of radio data are available for four separate wavelengths between 1.67 m and 4.18 m. Moreover, two radiosonde stations are located on or near the path, a unique situation in radiometeorological

TABLE 1.—Refractive index profile classification, probable propagation mechanisms and meteorological conditions

Profile	Assumed propagation mechanism	Reference	Meteorological conditions
Unstratified, (U) Monotonic decrease with height, gradient nowhere exceeds twice normal for that height.	Scattering plus diffraction.....	[Booker and Gordon, 1951].... [Villars and Weiskopf, 1954, 1955]. [Norton et al, 1955].	Well-mixed atmosphere due to thermal convection and, or wind shear.
Elevated Layer, (EL) Monotonic decrease with height with one or more distinct layers with gradients at least twice normal for that height.	Scattering plus Diffraction plus reflection.	[Smyth and Trolese, 1948]..... [Saxton, 1951]. [Misme, duCastel, Voge, 1960]	Layer formed by subsidence inversion or lifting of radiation inversion.
Super-Refractive, (SR) Same as EL but the layer is ground-based.	Extended radio horizon producing enhanced diffracted and scattered components.	[Norton et al, 1955].....	Radiation inversion formed during the night or rapid evaporation from soil after rain.
Ducting, (D) Same as SR but the gradient exceeds the earth's curvature, 1/a.	Extension of radio horizon to include the receiver.	[Booker-Walkinshaw, 1945]....	Same as SR.



FIGURE 1. Location of radio path and radiosonde stations used in this study.

investigations. Details of the radio paths are given in table 2 (in which  $\theta$  is the total angle between the horizon rays from transmitter and receiver on a 4/3-earth profile).

The meteorological data were obtained from the simultaneous radiosonde observations made by the Weather Bureau at Joliet and the Rantoul Air Force Base. The results used were those from the significant levels reported whenever the temperature or humidity departed by  $1^{\circ}\text{C}$  or  $\pm 10$  percent from predetermined values.

TABLE 2.—Chicago-to-Urbana radio path characteristics

Station	Distance	$\theta$	$\lambda$	$f$	Period of record
	km	mr	m	Mc/s	
WBKB-TV-----	203.1	16.3	4.18	71.75	5/51- 5/53
WNBQ-TV-----	202.9	16.7	3.67	81.75	10/50-10/51
WMBI-FM-----	202.7	16.1	3.15	95.50	7/50- 6/52
WENR-TV-----	202.9	16.4	1.67	179.75	7/51- 6/53

### 2.1. Classification of Radio Field Strengths by Profile Types

The RAOB significant level data were converted to refractive index by use of the Smith-Weintraub [1953] relationship

$$N = (n-1)10^6 = \frac{77.6}{T} \left( P + \frac{4810e}{T} \right) \quad (1)$$

where the pressure,  $P$ , temperature,  $T$ , and vapor pressure,  $e$ , are in the usual units of mb,  $^{\circ}\text{K}$ , and mb respectively. The gradient of  $N$  was then determined between the reported significant levels of each profile and examined as to whether the gradients fell into the category of linear, subrefractive or superrefractive depending upon the criteria set down in table 3 wherein superrefractive is approximately twice normal and subrefractive has a positive gradient. Simultaneous observations of similar profile types at Rantoul and Joliet were necessary for entry as a distinct profile occurrence. If a superrefractive layer occurred above the crossover heights of the radio horizon tangent rays from both transmitter and receiver, then it was classified as an elevated layer provided the reported layer heights were within 1 km of one another at both radiosonde stations. Elevated layers below the crossover height were classified as ground-based superrefractive layers. Elevated layers below the crossover height at one weather station and above that height at the other were classified as tilted elevated layers.

After these characteristic profiles were isolated, the median field strengths for the 3 hr period centered upon the radiosonde observation time were arranged into cumulative probability distributions for each profile type. The results are shown in figure 2. (There were relatively few examples of subrefractive profiles and no distributions for this category are given.) The 3-hr time interval about the 10 am and 10 pm CST radiosonde observation times was arbitrarily chosen to smooth the sometimes abrupt changes in signal characteristics observed during these transition periods of the diurnal cycle.

TABLE 3.  $N$  gradient classification of profile types in  $N$ -units/km

$P$	$h$	Sub-refractive	Unstratified	Super-refractive
mb	km			
1000-850	0 -1.46	$-\frac{dn}{dh} < 0$	$20 < -\frac{dn}{dh} < 60$	$100 < -\frac{dn}{dh}$
850-700	1.46-3.01	$-\frac{dn}{dh} < 0$	$20 < -\frac{dn}{dh} < 50$	$80 < -\frac{dn}{dh}$
700-600	3.01-4.20	$-\frac{dn}{dh} < 0$	$15 < -\frac{dn}{dh} < 40$	$70 < -\frac{dn}{dh}$
600-500	4.20-5.57	$-\frac{dn}{dh} < 0$	$10 < -\frac{dn}{dh} < 30$	$50 < -\frac{dn}{dh}$
500-400	5.57-7.18	$-\frac{dn}{dh} < 0$	$10 < -\frac{dn}{dh} < 25$	$40 < -\frac{dn}{dh}$

Generally, the unstratified samples have the lowest overall field strengths throughout the entire distribution range. The presence of any layer (elevated or ground-based) tends to increase the field strength by 10 to 25 db at any percentage level of the distribution. (The exception to this observation, WNBQ-TV, is probably explained by the fact that the observations were limited to six winter months, rather than the 2-yr period of the other stations.) Tilted elevated layers appear to produce the greatest enhancement of signal strength, probably as a result of focusing effects due to the layer tilt.

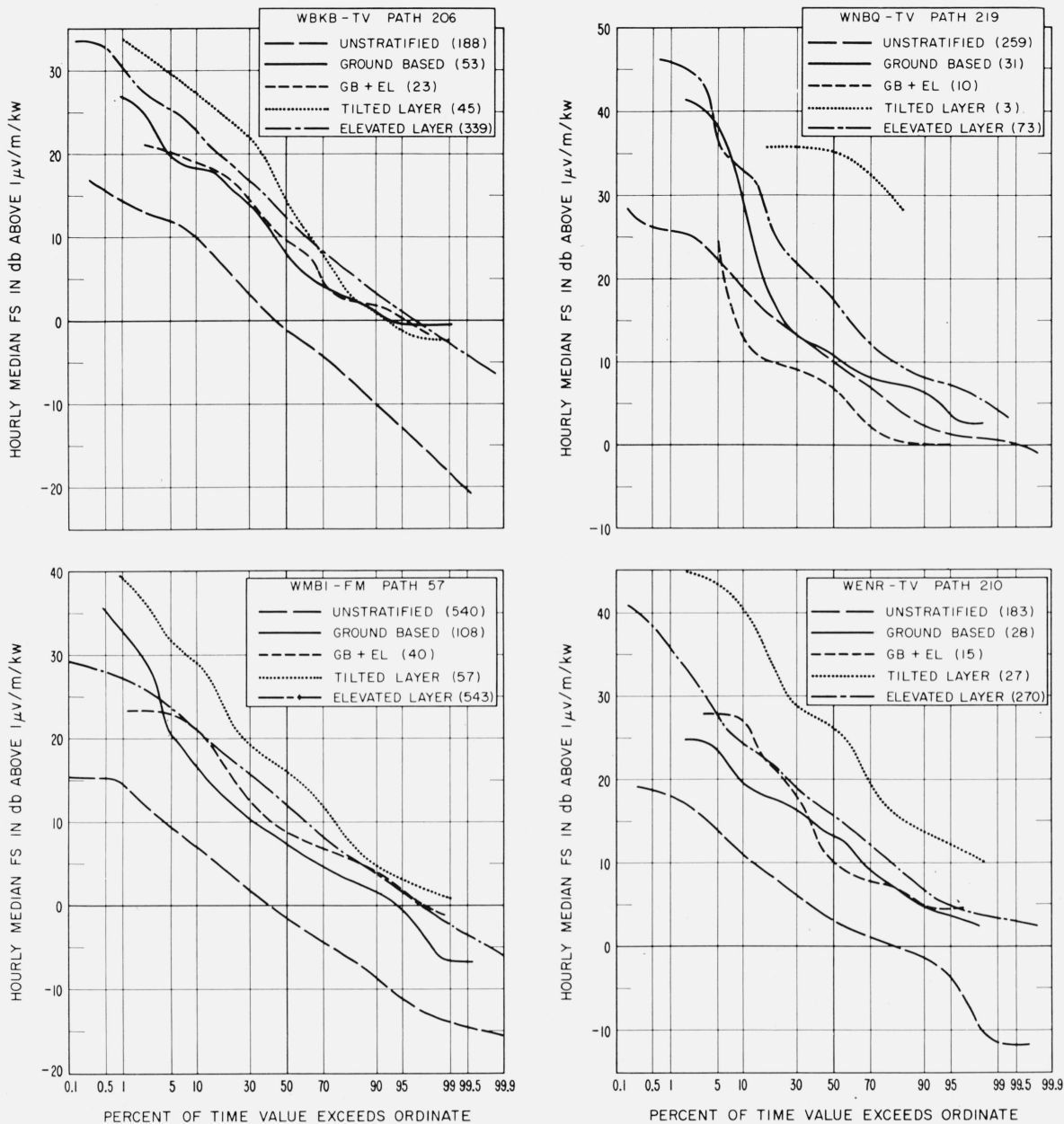


FIGURE 2. Distribution of hourly median field strengths with different radiosonde profile conditions.

## 2.2. Prediction of Field Strength for Unstratified Conditions

The field strengths recorded during the times when the radiosonde ascents at both Joliet and Rantoul indicated nonstratified conditions were compared with the values predicted by Norton, Rice, and Vogler [1955] for the case of diffracted plus scattered radio waves. This particular prediction process is adjustable for the average refractive conditions over the path in that it adjusts the effective earth's radius factor to the initial gradient of  $N$  for the calculation of diffracted field strengths. One also needs the angular separation of the radio

horizon rays at their intersection near midpath. The average initial gradient of  $N$  was obtained for each instance of unstratified profile by simply averaging the initial gradients from Rantoul and Joliet, while the angular separation was obtained by determining the amount of radio ray refraction expected over each particular path in atmospheres of exponential decrease with height that closely match the observed  $N$  conditions.

Figure 3 illustrates a comparison of the predicted and observed field strengths. For WNBQ and WENR there is approximate agreement between the two sets of data. However, the predicted values for WBKB and WMBI are approximately 10 to 12

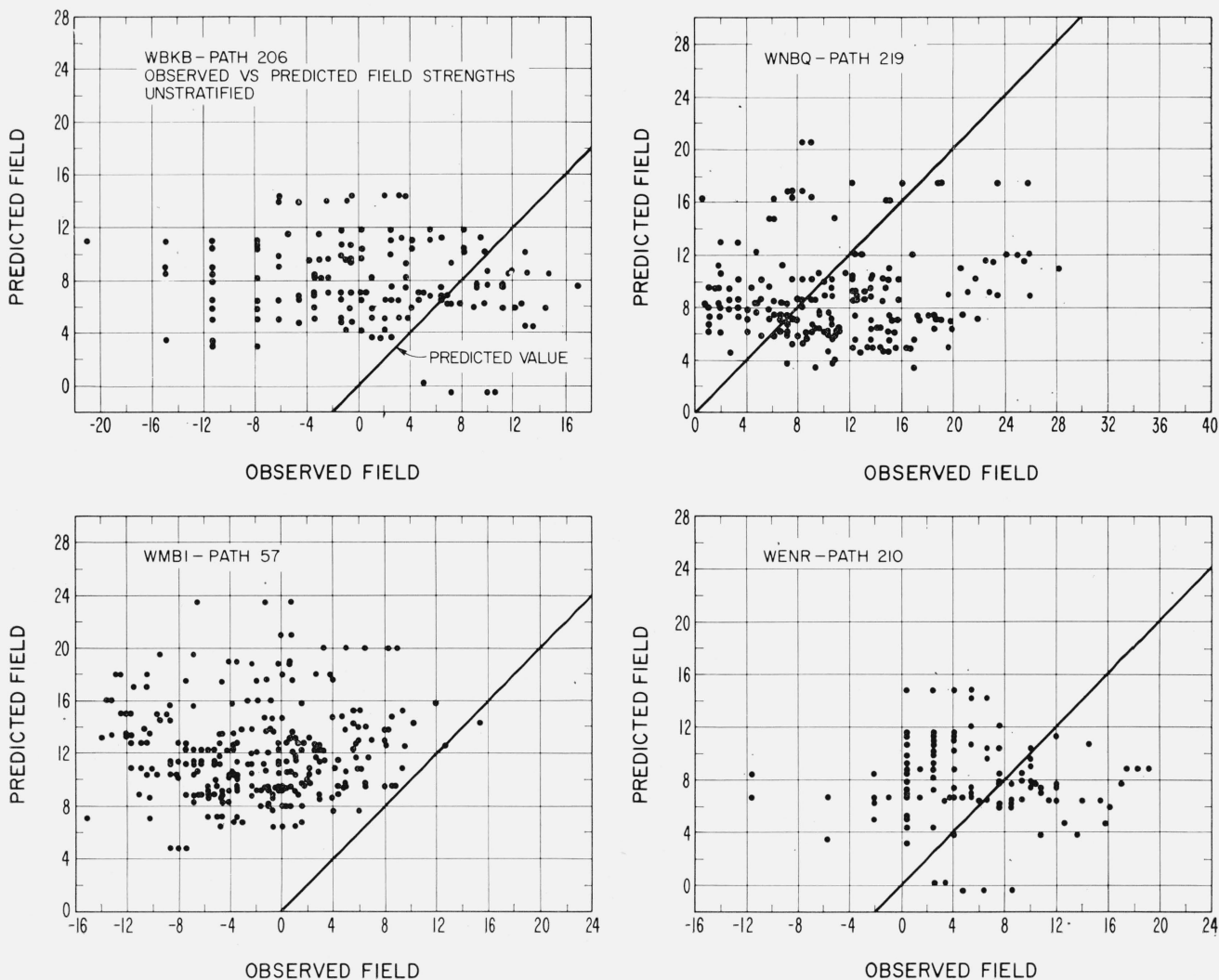


FIGURE 3. Comparison of observed radio field strengths and values predicted for wintertime afternoon hours.

db higher than the observed values. This tendency to predict fields in excess of the measured values suggests that the empirical data, on which the predictions are based, may include meteorological conditions with some degree of stratification, even though most of the empirical data refer to afternoon hours in winter. It will be shown in section 3.2 that elevated layers of moderate size (say a few kilometers in horizontal dimensions) may exist undetected by the radiosonde and could produce field strengths on the Illinois paths comparable with the median values for "unstratified" conditions shown in figure 2. Furthermore, the limits placed on the profile gradients specifying unstratified conditions in table 3 are such that some layer type profiles may be included in the unstratified category. Consequently, it is important to study in more detail the properties of the elevated layer, not only as a feature occasionally producing high field strengths, but also as a mechanism which, in less intense form, partly determines the strength of the weaker fields observed for large percentages of the time.

### 3. Effect of Elevated Layers on the Illinois Paths

The influence of elevated layers on VHF transmission beyond the horizon has been studied by several workers [Saxton, 1951; Gossard and Anderson, 1956; du Castel, Misme, and Voqe, 1960; Friis, Criawford, and Hogg, 1957; Starkey et al., 1958; Abld et al., 1952]. However, few investigations have contained any detailed comparisons of theory and experiment results. The following analysis presents such a comparison, using simple models of the elevated layer, for the four Illinois paths.

#### 3.1. Elevated Layers at Temperature Inversions

Recent radar and refractometer investigations of tropospheric structure have shown that elevated layers in the refractive index distribution are frequently observed in the stable air of temperature inversions [Lane and Meadows, 1963]. A typical value of layer thickness is 100 m, with horizontal dimensions of tens of kilometers. On occasions,

extended layers no more than 10 m in thickness have been detected by refractometer soundings. In the present discussion we attempt to evaluate the reflection coefficient of these elevated layers. We may express the modulus of the reflection coefficient  $|\rho|$ , for a wave incident at a glancing angle  $\alpha$  on a layer of thickness  $h$ , in the form:

$$|\rho| = \frac{\Delta n}{2\alpha^2} f(\alpha, h, x). \quad (1)$$

$f(\alpha, h, x)$  is the ratio of the reflection coefficient of the model to that of the infinitely sharp case (i.e., the Fresnel discontinuity value,  $\Delta n/a\alpha^2$ ). This function has been evaluated for several layer profiles [du Castel, Misme, and Voge, 1960], and preliminary calculations based on this work were made to determine the most suitable model in the present application. It was evident from these calculations that a simple linear profile would yield the best agreement with the measured data, and this model was therefore adopted in the subsequent analysis.

Consider the layer profile shown in figure 4, i.e., a linear decrease of  $n$  over a height interval  $h$ , with transition regions of height  $d$ . This model and others have been discussed by several authors, but the most detailed treatment is that of Brekhovskikh [1960.] His analysis shows that for this linear model:

$$\begin{aligned} |\rho| &= \Delta n \cdot \lambda / 8\pi h \sin^3 \alpha \\ &\simeq \Delta n \cdot \lambda / 8\pi h \alpha^3. \end{aligned} \quad (2)$$

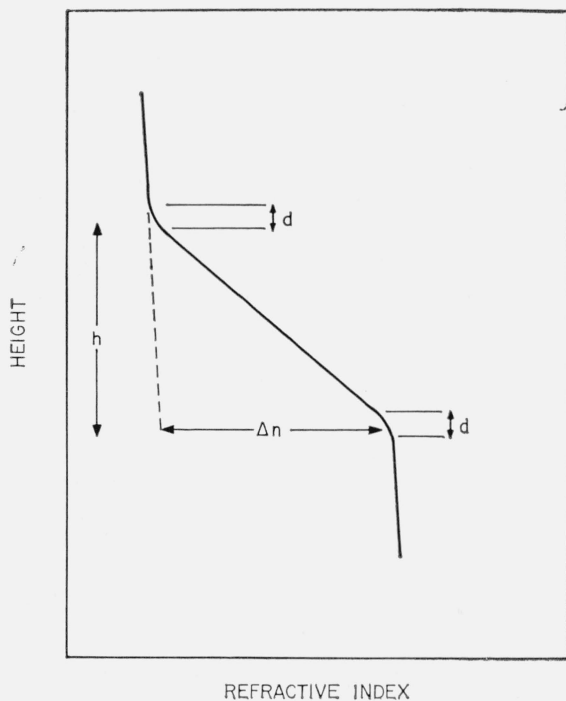


FIGURE 4. Linear profile model of the  $n$  decrease across an elevated layer.

This equation is valid if:

$$(a) \Delta n \cdot \lambda \ll \pi h \alpha^3$$

and

$$(b) 4\alpha d \ll \lambda.$$

In the present problem, with values of  $\lambda$  of 1.7 to 4.2 m,  $\alpha \sim 10^{-5}$ , condition (a) is satisfied for layer thicknesses greater than about 20 m. In addition, condition (b) is fulfilled for the stated conditions if the thickness of the transition region is less than a few meters. These conditions do not seem inconsistent with available refractometer data on elevated layers, but a rigorous justification of the model is impossible at the present time. In any case, there is almost certainly no unique profile representative of all elevated layers. We assume here, therefore, the linear profile of figure 4 merely as a simple analytical model. It may be noted here that the value of  $|\rho|$  given by (2) agrees with that quoted by du Castel [1961], but is half the value obtained in an earlier analysis [du Castel, Misme, and Voge, 1960].

Equation (2) was used to calculate the reflection coefficient of the layers on each occasion on which these were observed in the sonde ascents. The results, expressed in terms of a reflection loss, are compared with the measured values of field strength in figure 5. The general agreement is satisfactory for the assumed model. As might be expected, there is a considerable scatter in the data, and two considerations are important in assessing the significance of these results. These concern sonde response and layer structure. The work of Wagner [1960] on the response of radiosondes show that, for an elevated inversion layer with  $\Delta n = 3 \times 10^{-5}$ , and  $h = 100$  m, a sonde with a 10 sec time constant in the sensing elements, rising at 5 m/sec, will give an indicated value of  $\Delta n$  of approximately half the true value. The above procedure, using sonde data, therefore underestimates the value of  $|\rho|$  for an idealized infinite layer. On the other hand the analysis assumes a smooth layer extending horizontally at least over a distance  $x$  equal to the first Fresnel zone. We have:

$$x = \sqrt{2a\lambda}/2 \quad (3)$$

where  $2a = \text{path length} = 2-3$  km for the Illinois paths. Hence  $x$  is of the order of a few tens of kilometers. In addition, we have assumed that the layer is horizontal and smooth over a distance  $x$ , thus neglecting convergence. If we adopt the Rayleigh criterion, the height of the surface irregularities on the layer,  $\Delta h$  say, must not exceed  $\pm \lambda / 8\alpha$  for the layer to be considered smooth; i.e.,

$$\Delta h < \pm 7 \text{ m } (\lambda = 1.67 \text{ m}; f = 179.75 \text{ Mc/s})$$

$$\Delta h < \pm 17 \text{ m } (\lambda = 4.18 \text{ m}; f = 71.75 \text{ Mc/s}).$$

These values apply for  $\alpha = 0.03$  radian, corresponding to a layer height of 2.5 km; for lower layers  $\Delta h$  will be greater due to the decrease in  $\alpha$ .

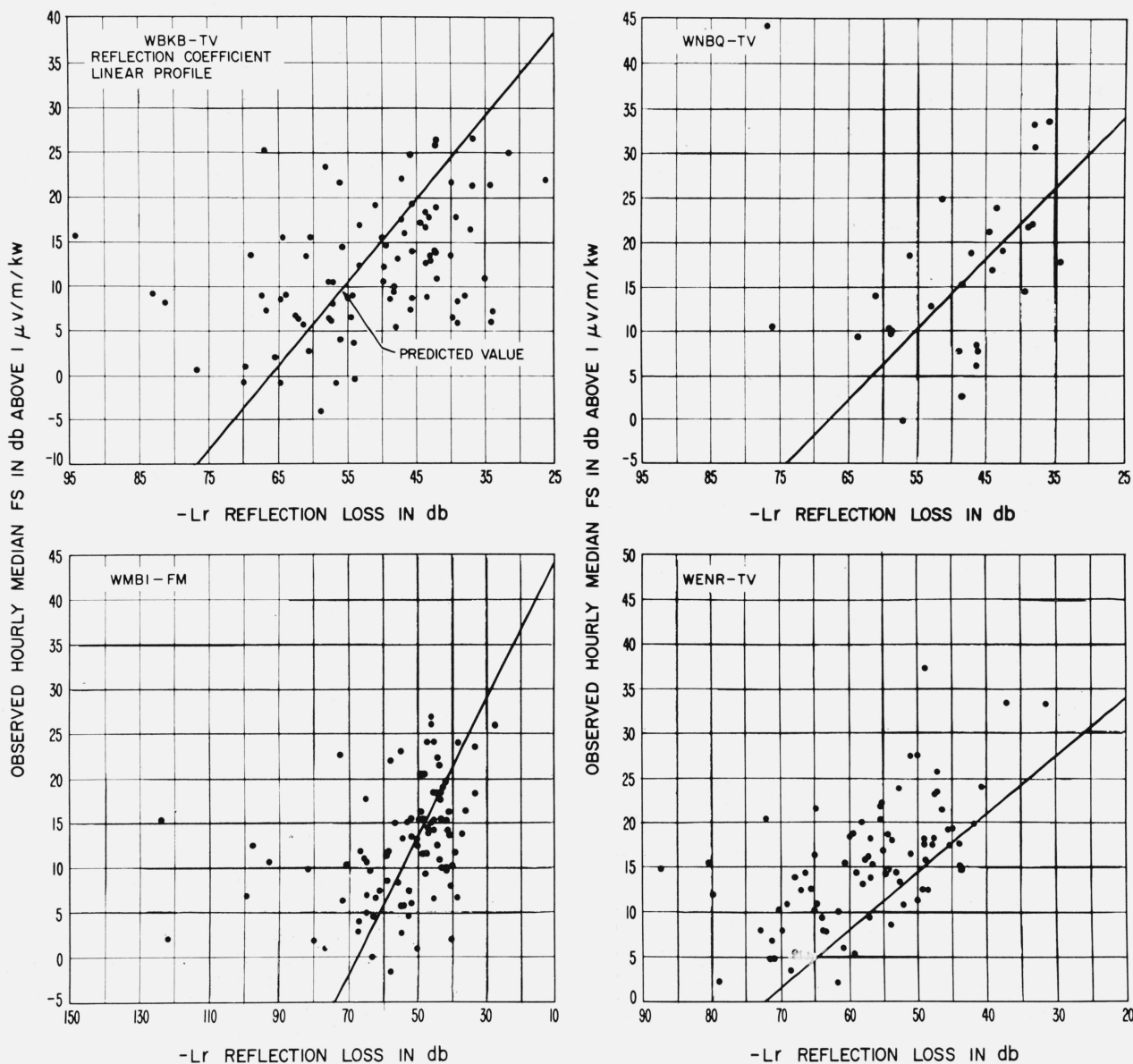


FIGURE 5. Observed hourly median field strength versus reflection loss assuming the linear model of figure 4.

These conditions are not likely to be satisfied in all the examples studied and the analysis therefore overestimates the value of  $|\rho|$  in this respect. (Some discussion of this point has been given by Bauer and Meyer [1958].) The limitations of sonde soundings, and the effects of layer tilt and surface irregularities therefore provide a partial explanation of the scatter of points in figure 5. Further detailed measurements of layer structure are obviously desirable.

### 3.2. Influence of Small Layers

The above discussion has dealt with the particular case of extended elevated layers such as are often associated with temperature inversions. However, it seems quite possible that these layers are merely the more extreme examples of anisotropic irregu-

larities which are thought to be prevalent in the troposphere. There is already some preliminary evidence supporting this concept in the results of refractometer and radar soundings [Lane and Meadows, 1963; Saxton, 1960], and recent theoretical work [du Castel, Misme, and Voge, 1960; Friis, Crawford, and Hogg, 1957; du Castel, 1961] has developed this approach in detail. The relationship of this work to earlier analyses in terms of a "scattering" model is discussed in the references quoted and need not concern us here. For our purpose it is sufficient to utilize the essential features of the argument as the basis for a simple calculation.

It seems reasonable to assume that even in an atmosphere which sonde data would lead us to classify as "well mixed" there are often layer-type irregularities. Detailed evidence on the spatial form and stability of this type of layer or "feuillet"

is so far lacking, but an inspection of some refractometer results suggests that horizontal dimensions of a few kilometers represent a realistic assumption. Such a layer might exist as a separate entity for say several minutes (as compared with a period of several hours for the extended layer in a stable inversion).

For the following analysis, let us consider two layers of horizontal dimensions,  $x$ , of 2 and 10 km respectively with the following characteristics:

$$\Delta n = 10^{-5}$$

$$h = 100 \text{ m}$$

$$\alpha = 0.01\text{--}0.03 \text{ radian (i.e., layer height of 0.4\text{--}2.5 \text{ km on the Illinois paths).}$$

For these conditions, the layers correspond to those of "intermediate" size in the analysis of Friis, Crawford, and Hogg. They are defined by the equation:

$$\sqrt{2a\lambda/\alpha} > x > \sqrt{2a\lambda} \quad (4)$$

where  $2a$  is the path length. In this case, the power received,  $P_R$ , from an antenna of effective aperture,  $A_R$ , with a transmitter radiating a power  $P_T$  from an antenna of effective aperture  $A_T$  is given by:

$$P_R/P_T = (A_T A_R \lambda^2 \alpha^2 \rho^2) / (2\lambda^3 a^3). \quad (5)$$

We can use this equation to calculate the corresponding field strength, for the Illinois paths, in terms of  $\mu\text{V}/\text{m}$  for 1 kw radiated from a half-wave dipole. We have the following relations:

$$A(\lambda/2 \text{ dipole}) = 0.127\lambda^2 \quad (6)$$

$$P_R(\lambda/2 \text{ dipole}) = E^2\lambda^2/300\pi^2 \quad (7)$$

where  $E$  is the field strength in volts/meter if  $P_R$  is in watts. From (5), (6), and (7) we can calculate  $E$  for the two layers specified above, and the results obtained are shown in figure 6 for various layer heights and the following models of reflection coefficient:

$$(a) |\rho| = \Delta n \cdot \lambda / 8\pi\alpha^3 h$$

$$(b) |\rho| = \Delta n / 2\alpha^2$$

Model (b) is the Fresnel discontinuity equation which gives the limiting value of  $|\rho|$  toward which all models tend as the layer thickness decreases. The curves in figure 6 show that the calculated field strength depends considerably on the assumed  $n$ -profile. If  $|\rho| = \Delta n \cdot \lambda / 8\pi\alpha^3 h$ , values of field strength comparable with the long-term median value may be produced by layers of about 10 km in lateral dimensions in the height range 0.5–1 km. If  $|\rho| = \Delta n / 2\alpha^2$ , similar field strength may be produced by layers in this height range if the lateral dimension is of the order of 2 km. The effect of the layer decreases with increasing height, but even with layer heights of 3 km, the field strength is still  $1 \mu\text{V}/\text{m}$  or greater at both wavelengths for a 10 km layer with  $|\rho| = \Delta n / 2\alpha^2$ . However, it should be pointed out that the assumed value of  $\Delta n = 10^{-5}$  is probably

somewhat large for layers as high as 3 km. The results also show that model (b) (i.e.,  $\rho = \Delta n / 2\alpha^2$ ) gives field strength values which are higher at  $\lambda = 1.67 \text{ m}$  ( $f = 179.75 \text{ Mc/s}$ ) than at  $\lambda = 4.18 \text{ m}$  ( $f = 71.75 \text{ Mc/s}$ ).

The distribution of wavelength dependence is further illustrated in figure 7. The hourly median values of field strength (or transmission loss,  $L$ ) at times of the sonde ascents were used to derive the wavelength dependence as a function of refractive index profile characteristics. Here, transmission loss is defined by  $p\alpha/p\gamma$ , where:

$p\alpha$  = Available power at the terminals of a loss-free antenna.

$p\gamma$  = Power radiated from the transmitting antenna.

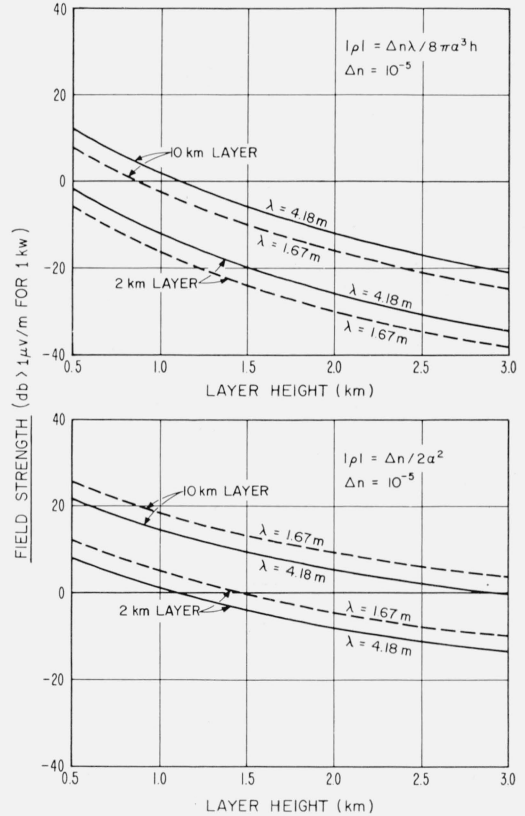


FIGURE 6. Field strength produced by layers of horizontal dimensions 2 km and 10 km on Chicago-Urbana paths for two model profiles.

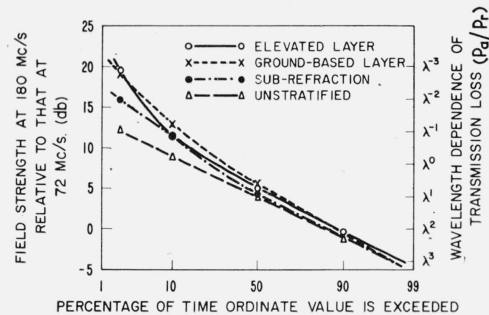


FIGURE 7. Wavelength dependence on Chicago-Urbana path as a function of time and season.

The wavelength dependence varies considerably, even in any one profile category; this result further emphasizes the complexity of the propagation mechanism on a VHF path of intermediate length (~200 km). A full discussion of this problem is outside the scope of this paper, but it seems probable that all of the following features are important in determining the range of wavelength dependence:

- (a) Occasional deep surface or elevated ducts, giving enhancements of the 180 Mc/s signal,
- (b) the different profile characteristics of elevated layers, as illustrated by the results of figure 6;
- (c) the path geometry,
- (d) elevated layers or large anisotropic eddies which are not detected by the radio sondes.

It seems likely that the weakest fields measured on the Illinois paths are produced by a diffracted component. The wavelength dependence in such a situation has been discussed by Schelleng, Burrows, and Ferrell [1933], who drew attention to enhancements of the higher frequency field strength, on a two-channel VHF path, resulting from the path geometry and consequent antiphase interference between ray paths at the lower frequency. Omitting the extreme categories of (a) weak diffracted fields, and (b) fields influenced by deep ducts, the range of wavelength dependence indicates the possible effect of a distribution of layer sizes with varying surface roughness and  $n$ -profile. Even in an apparently "well-mixed" atmosphere there is rarely a unique propagation mechanism on this 200 km path in the frequency range 70 to 180 Mc/s, a conclusion consistent with the results of figure 3.

#### 4. Conclusions

Any departure of refractive index structure from a smooth monotonic decrease with height produces an increase in field strength on a 200-km path in the frequency band 70 to 180 Mc/s. In the particular case studied, elevated tilted layers result in signal enhancements of 10 to 25 db, over the values for unstratified conditions, at all percentage levels. (The importance of the tilted layer is possibly a consequence of the asymmetry of the path, the transmitting antenna being 200 m above ground and the receiving antenna 30 m.)

The predicted field strengths, for conditions classified as unstratified in terms of sonde data, are in approximate agreement with observed results, although the scatter of the points (plus the tendency to predict values in excess of the measured ones) point to the influence of anisotropic layers or eddies of varying size and degree of stability. This interpretation is consistent with numerical calculations based on the properties of "intermediate" size layers,

suggested in the analysis of Friis, Crawford, and Hogg [1957].

Calculations of the field strength produced by extended stable layers, using sonde data and a model profile with a linear lapse of  $n$  with height, are in reasonable agreement with the experimental results. However, there is probably no unique profile characteristic of elevated layers.

The present work has grown out of a study initiated some ten years ago by J. W. Herbstreit. His early guidance is greatly appreciated.

#### 5. References

- Abild, V. B., H. Wensien, E. Arnold, and W. Schiloski (May-June 1952), Über die ausbriertung ultrakurzer wellen jenseits des horizontes unter besonderer beruicksichtigung der meteorologischen einwirkungen, Tech. Hausmitteilungen des Nordwestdeutschen Rundfunks, p. 85.
- Bauer, J. R., and J. H. Meyer (1958), Microvariations of water vapor in the lower troposphere with applications to long-range radio communications, Trans. Am. Geophys. Union **39**, 624.
- Booker, H. G., and W. E. Gordon (1950), A theory of radio scattering in the troposphere, Proc. IRE **38**, 401.
- Brekhovskikh, L. M. (1960), Waves in layered media (Academic Press, New York and London).
- duCastel, F., P. Misme, and J. Voqe (1960), Sur le role des phenomenes de reflexion dans las propagation loutaine des ondes ultracourtes, Electromagnetic Wave Propagation, p. 671 (Academic Press, London and New York).
- duCastel, F., (1961), Propagation tropospherique et faisceaux hertziens transhorizon, p. 90 (Editions Chiron, Paris).
- Friis, H. T., A. B. Crawford, and D. C. Hogg (1951), A reflection theory for propagation beyond the horizon, Bell System Tech. J. **36**, 627.
- Gossard, E. E., and L. J. Anderson (1956), The effect of super refractive layer on 50-5000 Mc non-optical fields, IRE Trans. Antennas and Propagation **AP-4**, No. 2, 175-178.
- Lane, J. A., and R. W. Meadows (1963), Radar and refractometer soundings of the troposphere, Nature **197**, 35.
- Norton, K. A., P. L. Rice, and L. E. Vogler (1955), Use of angular distance in estimating transmission loss and fading range for propagation through a turbulent atmosphere over irregular terrain, Proc. IRE **43**, 1488.
- Saxton, J. A. (1951), Propagation of metre radio waves beyond the normal horizon, Proc. IEE **98**, pt. III, 360-369.
- Saxton, J. A. (1961), Quelques reflexions sur la propagation des ondes radioelectrique a travers la troposphere, L'Onde Elect. **40**, 505.
- Schelleng, J. C., C. R. Burrows, and E. R. Ferrell (1933), Ultra short wave propagation, Proc. IRE **21**, 427.
- Smyth, J. B., and L. G. Trolese (1947), Propagation of radio waves in the lower atmosphere, Proc. IRE **35**, 1198.
- Starkey, B. J., W. R. Turner, S. R. Badcoe, and G. F. Kitchen (1958), The effects of atmospheric discontinuity layers up to the tropopause height on beyond-the-horizon propagation phenomena, Proc. IEE pt. B, **105**, supp. 8, 122.
- Villars, F., and V. F. Weisskopf (1955), On the scattering of radio waves by turbulent fluctuations of the atmosphere, Proc. IRE **43**, 1232.
- Wagner, N. K. (1960), An analysis of radio-sonde effects on measured frequencies of occurrence of ducting layers, J. Geophys. Res. **65**, 2077.

(Paper 67D6-292)